Stoichiometry Studies Reveal Functional Properties of KDC1 in Plant *Shaker* Potassium Channels

Alessia Naso, Roberta Montisci, Franco Gambale, and Cristiana Picco
Istituto di Biofisica, Consiglio Nazionale delle Ricerche, Genoa, Italy

ABSTRACT Functional heteromeric plant *Shaker* potassium channels can be formed by the assembly of subunits from different tissues, as well as from diverse plant species. KDC1 (K^+ *Daucus carota* 1) produces inward-rectifying currents in *Xenopus* oocytes when coexpressed with KAT1 and other subunits appertaining to different plant *Shaker* subfamilies. Owing to the presence of KDC1, resulting heteromeric channels display slower activation kinetics, a shift of the activation threshold toward more negative membrane potentials and current potentiation upon the addition of external zinc. Despite available information on heteromerization of plant *Shaker* channels, very little is known to date on the properties of the various stoichiometric configurations formed by different subunits. To investigate the functional properties of heteromeric nKDC1/mKAT1 configurations, we realized a series of dimeric constructs combining KDC1 and KAT1 α-subunits. We found that homomeric channels, formed by monomeric or dimeric α-subunit constructs, show identical biophysical characteristics. Coinjections of diverse tandem constructs, instead, displayed significantly different currents proving that KDC1 has high affinity for KAT1 and participates in the formation of functional channels with at most two KDC1 subunits, whereas three KDC1 subunits prevented the formation of functional channels. This article brings a contribution to the understanding of the molecular mechanisms regulating plant *Shaker* channel functionality by association of modulatory subunits.

INTRODUCTION

In animal as well as in plant cell membranes, potassium channels are tetramers formed in the endoplasmic reticulum from four identical or different subunits, transferred to the plasma membrane as homomeric or heteromeric channels, which are irreversibly assembled (1–11). Evolution selected a series of modulatory auxiliary α- or β-subunits to fine-tune the ion channels properties according to cellular needs (12). Unlike β-subunits, modulatory α-subunits participate in the formation of the channel's permeation pore. They possess properties of auxiliary regulatory proteins and play modulatory roles in either voltage- (13–15) or ligand-gated channels (16–20). While modulatory α-subunits participate in the formation of heteromeric channels, they are typically unable to form functional homotetrameric channels when expressed alone in heterologous systems.

The stoichiometry of voltage-dependent potassium channels has been extensively described in animal cells (2,15,21,22). For example, the stoichiometry of heteromeric potassium channels composed of animal Kv2.1 and the modulatory Kv9.3 (23) α-subunits was recently resolved by FRET measurements (15). These channels heteromerize with a fixed 3:1 stoichiometry between α-subunits and a modulatory α-subunit; similar results were obtained for CNG channels (24).

Differently from animal channels, no information is available to date on the assembly and the functional properties of different stoichiometric configurations of potassium channels in plants. KDC1 (from *Daucus carota*) is a plant *Shaker*-type subunit belonging to the silent AtKC1 group, which does not express functional homomeric channels in *Xenopus* oocytes (7,11). It has been demonstrated that KDC1 participates in the formation of stable inward-rectifying potassium channels when coinjected with other potassium channel subunits cloned from carrot (like DKT1 (25)) or from other plants (7,11). KAT1 (from *Arabidopsis thaliana*) belongs to group II of plant *Shaker* channels (26,27) (for review, see (28,29)). While DKT1 properties are unknown (as DKT1 does not express functional homomeric channels in oocytes (25)), KAT1 is a well-characterized channel producing stable currents when coinjected with KDC1, therefore it is a useful partner for coexpression with KDC1. Interestingly, the presence of KDC1 slows the activation of inward currents down and shifts the threshold of activation toward more negative membrane potentials. Moreover, KDC1 also modifies the current response to Zn^{2+} added to the bath solution: indeed, contrary to KAT1, heteromeric channels comprising KDC1 are no longer inhibited, but rather potentiated by external zinc (7,11). Zinc binding involves two histidines residing in the KDC1 S3–S4 and S5–S6 linkers (11). This peculiar reactivity of KDC1 to zinc can be used as a pharmacological tool to monitor the presence and properties of KDC1 in heteromeric K^+ channels.

The interaction of KDC1 with KAT1 subunits was investigated by the coinjection of KDC1 and KAT1 constructs in

Submitted June 20, 2006, and accepted for publication August 3, 2006.

Address reprint requests to Cristiana Picco, Tel.: 39-0-10-647-5569; E-mail: picco@ge.ibf.cnr.it.

Abbreviations used: KDC1:KAT1, coinjection of KDC1 and KAT1; KDC1-KAT1, dimeric construct made by KDC1 and KAT1; KDC1-KDC1:KAT1-KAT1, coinjection of two dimeric constructs, in this case KDC1-KDC1 and KAT1-KAT1; nKDC1/mKAT1, stoichiometric configuration comprising *n*-KDC1 and *m*-KAT1.

0006-3495/06/11/3673/11 $2.00

doi: 10.1529/biophysj.106.091777

Xenopus oocytes, with the aim to verify which stoichiometric configuration, between these two subunits, is functional.

As the assembly of tetrameric channels seemed to proceed as a dimerization of dimers (30), we decided to coinject a series of appropriate tandem constructs encoding for covalently linked KAT1 and KDC1. This allowed us to decrease the number of possible configurations originating from the combination of different subunits, and to facilitate the interpretation of coexpression experiments (Fig. 1).

MATERIALS AND METHODS

Molecular biology

Dimeric constructs schematically represented in Fig. 1 were obtained as follows.

KAT1-KAT1 dimeric construct

Vector: KAT1 inserted in pGEMHE vector (5) was mutated at the 5′ end of the coding sequence to insert a *Bam*HI site.

Insert: After the above modification, the vector was also mutated at the 3′ end of the coding sequence of KAT1 to insert a *Bam*HI site. Vector and insert were digested with *Bam*HI and a ligation was performed to ligate KAT1 insert in KAT1-pGEMHE vector. The tandem construct was analytically digested to verify the correct orientation of the insert, then positive clones were sequenced to assess that the right reading frame between the two coding sequences was maintained. Three amino acids were inserted to link the C- and N-termini of KAT1 which remained otherwise unaltered; a similar procedure was also adopted to construct other dimers (see below).

KDC1-KDC1 dimeric construct

Vector: KDC1-pGEMHE was mutated to insert a *Sac*II site at the 5′ end of the coding sequence of KDC1.

Insert: KDC1 cDNA was amplified by PCR from KDC1-pGEMHE to insert a *Sac*II site both at the N-terminus and C-terminus eliminating the stop codon. Amplified KDC1 (1.7 Kb) and KDC1-pGEMHE were digested with *Sac*II, and KDC1-pGEMHE was subsequently digested with *Sma*I in the region before the start codon; in this way a 23-bp region was deleted, eliminating an ATG codon to avoid an incorrect starting point. The two fragments were ligated by T4 DNA ligase at the *Sac*II site. After EtOH-precipitation, T4 DNA polymerase was used to blunt the nonligated-*Sac*II-digested ends of amplified KDC1, and a second ligation was performed to close the KDC1-pGEMHE, with inserted KDC1, using *Sma*I-generated blunt end. The dimeric construct was analytically digested to verify the correct orientation of the insert, and then positive clones were sequenced to check the presence of the correct frame between the two coding sequences.

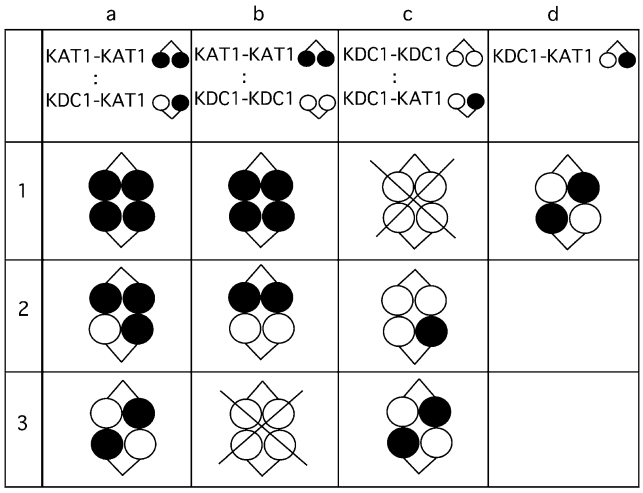

FIGURE 1 Schematic representation of various configurations generated by the coinjection of dimeric constructs. Different hypothetical configurations produced by coinjections of KAT1-KAT1, KDC1-KDC1, and KDC1-KAT1 tandem constructs at 1:1 cRNA ratio. Note that the homomeric KDC1 channel is not functional.

KDC1-KAT1 dimeric construct

See Picco et al. (11) for details.

Mutated KDC1$_{G226A}$-KDC1$_{G266A}$ dimeric construct

Vector: KAT1-KDC1 tandem (not described) was mutated in the pore region of the KDC1 sequence by site-directed mutation of glycine 266 into an alanine (G266A).

Insert: Monomeric KDC1$_{G266A}$ was amplified by PCR to introduce a *Sac*II recognition site both at the N-terminus and C-terminus eliminating the stop codon. KAT1-KDC1$_{G266A}$ and KDC1$_{G266A}$ were digested with *Sac*II. KAT1-KDC1$_{G266A}$ digestion produced two fragments of 2000 bp (KAT1) and 5000 bp (pGEMHE-KDC1$_{G266A}$), respectively. KAT1-KDC1$_{G266A}$ *Sac*II-digested and KDC1$_{G266A}$ *Sac*II-digested were loaded on a preparative agarose gel, and the two bands obtained from KAT1-KDC1$_{G266A}$ digestion were separated. The 5000 bp and the KDC1$_{G266A}$ *Sac*II-digested bands were eluted from the gel. The two fragments were then ligated by T4 DNA ligase using the *Sac*II site. The tandem construct was analytically digested to verify the correct orientation of the insert, and then positive clones were sequenced to check the correct frame between the two coding sequences.

Mutations were obtained using QuikChange Site-Directed Mutagenesis Kit (Stratagene, La Jolla, CA). All mutants were sequenced to confirm the mutation. PCR amplifications were performed with a Tpersonal thermocycler (Biometra, Gottingen, Germany), using Advantage 2 PCR Kit (Clontech, Mountain View, CA). Restriction enzymes were from Fermentas (Burlington, Ontario, Canada) or Promega (Promega, Milano, Italy). In vitro transcription was performed using the mCAP-RNA Capping Kit (Stratagene).

Oocyte expression and electrophysiology

Oocytes were isolated from *Xenopus laevis* females (31) and injected or coinjected (at 1:1 weight ratio, unless otherwise specified) with cRNA (0.4 μg/μl) encoding for wild-type and mutant homomeric and dimeric constructs using a Drummond ''Nanoject'' microinjector (50 nl/oocyte). Whenever a comparison was made, experiments were performed on the same batch of oocytes, from the same frog, and always on the same day from the injection. Whole cell K^+ currents were measured with a two-microelectrode homemade voltage-clamp amplifier (designed by F. Conti), using 0.2–0.4 MΩ electrodes filled with 3 M KCl. The following standard bath solution was used (in mM): 100 KCl, 2 $MgCl_2$, 1 $CaCl_2$. 1 $LaCl_3$, and 10 MES/Tris, pH 5.6. 1 mM $LaCl_3$ was added to the bath solution to inhibit oocyte endogenous currents elicited by potentials more negative than −160 mV. It was verified in advance that in our working conditions La^{3+} had no effect on the K^+ channels under investigation (C. Picco, A. Naso, P. Soliani, and F. Gambale, unpublished). Zn^{2+} was added to the external standard solution as $ZnCl_2$ at 1 mM concentration.

Data analysis

The relative open probability was obtained by dividing the steady-state currents by (V-V_{rev}) and was normalized to the saturation value of the

calculated Boltzmann distribution. Unless otherwise indicated, experimental points represent mean values of at least five experiments, mean ± SE. Half-activation potentials ($V_{1/2}$) and apparent gating charge, z, were determined by fitting experimental points with a single Boltzmann isotherm of the form: $P_{open} = 1/[1 + \exp(zF(V\text{-}V_{1/2})/RT)]$.

The binomial distribution $\Phi_i = n!/[i!(n–i)!] * \theta^i(1–\theta)^{n-i}$ (where Φ_i is the fraction of protein containing i subunits, θ is the molar fraction of the X-subunit, and n is the number of subunits participating to the channel) was used to calculate the probability of random and independent tetramer formation from two (X and Y) dimers (21).

RESULTS

KDC1 has modulatory capability and high affinity for other inward-rectifying plant *Shaker* K^+ channel subunits

KDC1 from carrot is an efficient modulator of plant inward-rectifying K^+ channel subunits, like KAT1, modifying some of the characteristics such as the activation threshold and the kinetics of channel activation (Fig. 2 *A*, *right*). It has also been demonstrated that an increased percentage of KDC1, coinjected with KAT1, determines a progressively slower current activation and an increased sensitivity to current potentiation mediated by zinc (7,11). Notably, KDC1 also favors the functional expression of potassium channel subunits, which do not produce functional homomeric channels in *Xenopus* oocytes (32–34). As illustrated in Fig. 2 *A* (*left*), KDC1 was able to form fully functional ion channels with DKT1 (also from carrot) (25), SKT1 (from *Solanum tuberosum*), and AKT1 (from *A. thaliana*) when coinjected (at 1:1 weight ratio). Consistently with what was observed on KDC1:KAT1 (7,11), these inwardly directed currents were mediated by heteromeric channels which displayed properties related to KDC1 such as zinc-dependent potentiation of the current (25).

The high affinity of KDC1 for other potassium channel subunits, irrespectively of the plant origin, is exemplified in Fig. 2 *B*, where the coinjection of the mutated nonfunctional KDC1 form ($KDC1_{G266A}$ mutated in the pore segment (35)) determined a dramatic 100-fold decrease of the expected KAT1 current. Under the hypothesis that the dimers associate randomly, the expected value of KAT1 currents for a binomial distribution would be 1:16 of the KAT1 control (see Materials and Methods). Interestingly, the decrease of the current to 1:100, with respect to the KAT1 control, suggests a nonbinomial association between KDC1 and KAT1.

To obtain more information on the modulatory capability of KDC1, we thought it would be useful to examine the functional properties of configurations comprising different KDC1 stoichiometric ratios. Therefore, we realized homo- and hetero-dimeric constructs made of either KDC1 or KAT1, as well as of both subunits.

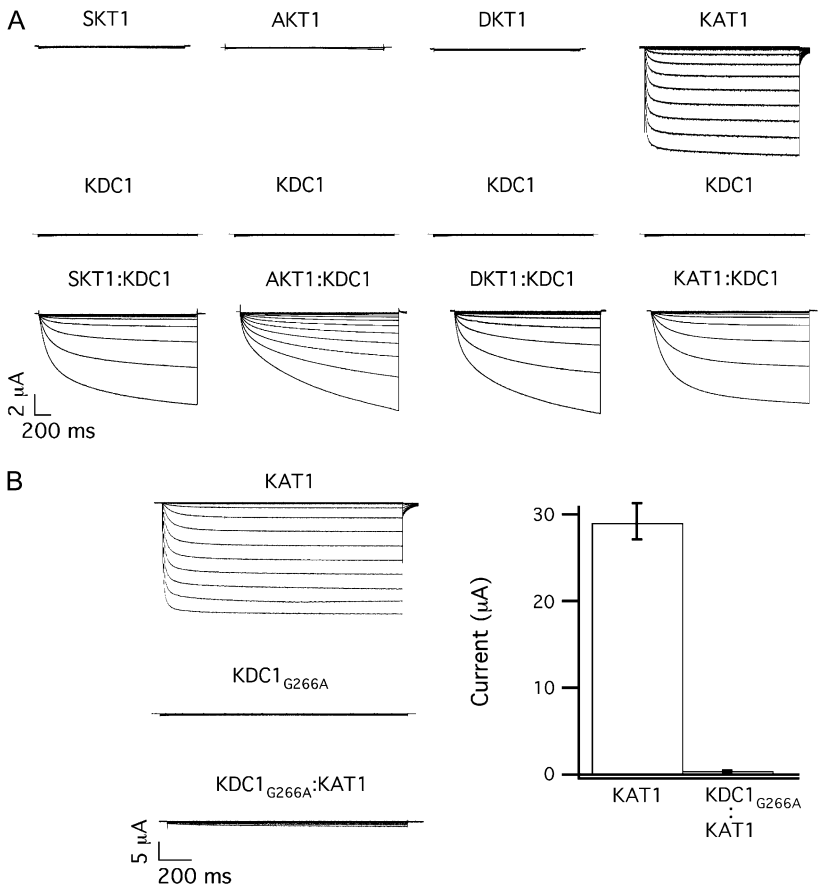

FIGURE 2 KDC1 has strong affinity and modulatory capability when injected with other inward-rectifying subunits in *Xenopus* oocytes. (*A*) Typical ionic currents recorded after the injection of KDC1 (*middle*) or SKT1, AKT1, DKT1, and KAT1 (*top* from *left* to *right*) and by coinjection of KDC1 with the correspondent inward rectifying partner (*bottom*); data are representative of at least five experiments for each coinjections. (*B*) Glycine 266 was mutated into alanine in KDC1 pore and the mutated $KDC1_{G266A}$ was injected at a 1:1 weight ratio with wild-type KAT1. It can be observed that $KDC1_{G266A}$ strongly decreases the probability of occurrence of KAT1 homomers. Left typical currents, right mean currents ± SE of 12 experiments. Applied membrane potentials are from 0 mV to −240 mV in –20 mV steps; holding and tail potentials are 0 mV and −50 mV.

Characteristics of homomeric channels formed by KDC1 and KAT1 dimers

The tandem construct KAT1-KAT1 injected in oocytes showed current activation properties almost undistinguishable from those produced by monomeric KAT1 (Fig. 3, *A*, *D*, and *E*). More specifically, the open probability characteristics of homomeric channels composed by monomeric and dimeric constructs (Fig. 3 *E*) displayed comparable half-activation potentials, $V_{1/2}$, and apparent gating charges, z: i.e., $V_{1/2}(KAT1_{\text{monomer}}) = -121.9 \pm 0.9$ mV and $V_{1/2}(KAT1_{\text{dimer}}) = -123.4 \pm 0.9$ mV, while $z(KAT1_{\text{monomer}}) = 1.4 \pm 0.7$ and $z(KAT1_{\text{dimer}}) = 1.4 \pm 0.6$ (see Table 1).

We used zinc as a molecular tool to further investigate the similarities of KAT1 channels obtained from KAT1 monomers and dimers. The addition of 1 mM $ZnCl_2$ to the bath solution induced a comparable inhibition of channels expressed by the two constructs (Fig. 3 *B*) (see also (11)).

Similarly to the KDC1 monomeric subunit, the dimeric KDC1-KDC1 construct did not form homomeric functional channels when injected in oocytes (Fig. 3, *C* and *D*). Therefore, we conclude that the expression of tandem (KDC1 or KAT1) constructs produced channels undistinguishable from those produced by the monomeric subunits.

Characteristics of the currents elicited by the coinjection of KDC1 and KAT1 homo- and hetero-dimeric constructs

On this basis, we coinjected the tandem constructs schematically represented in Fig. 1 and investigated the properties of KDC1 and KAT1 heteromeric channels. The different coinjections will be named hereafter coinjection **a**, **b**, or **c**, and the stoichiometric configurations will be indicated as case **a1**, **b1**, **c1**, **a2**, etc., according to the scheme illustrated in Fig. 1. We finally refer to KDC1-KAT1 injection as injection **d** or case **d1**. It is worthwhile to mention that earlier studies on tetramerization of A-B dimers already demonstrated that dimers pair up in an ABAB fashion, and that the formation of functional channels, where half of the dimer is left outside the channel core, is an improbable event (2,36–38).

When the dimeric constructs KAT1-KAT1, KDC1-KAT1, and KDC1-KDC1 were coinjected in different combinations,

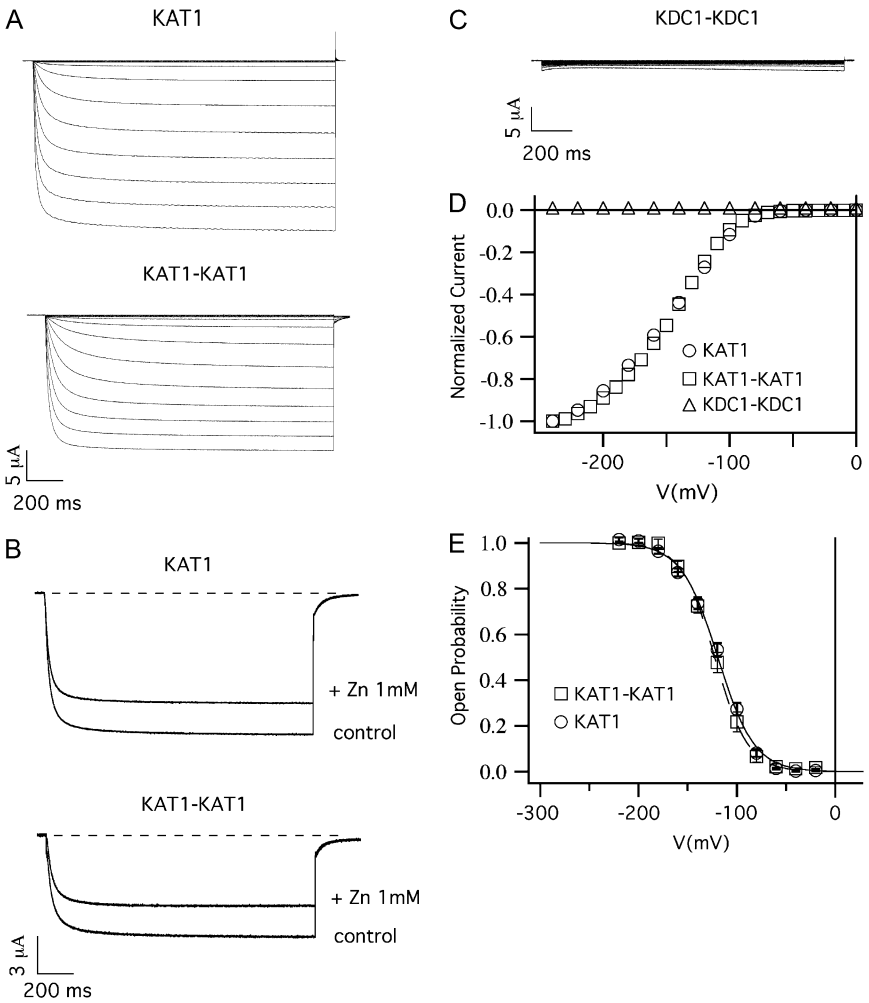

FIGURE 3 KAT1-KAT1 dimer (but not KDC1-KDC1 dimer) forms functional channels. (*A*) Functional expression of the KAT1-KAT1 dimeric construct. Ionic currents elicited by voltage steps from 0 mV to –240 mV in –20 mV decrements from a holding potential of 0 mV in oocytes injected with KAT1 and KAT1-KAT1 tandem constructs. (*B*) Inhibition of the current for the KAT1 and KAT1-KAT1 subunits, on the addition of 1 mM of $ZnCl_2$ to the bath solution. Holding, step, and tail potential are, respectively, 0 mV, −160 mV, and –50 mV. (*C*) *Xenopus* oocytes injected with KDC1-KDC1 tandem and stimulated with the same potential protocol used in panel *A* did not display any current. (*D*) Current voltage characteristics of the current families in panels *A* and *C* were normalized to the steady-state currents at –240 mV and plotted as a function of the applied voltage. (*E*) Open-probability characteristics of the KAT1 monomeric and KAT1-KAT1 dimeric channels. Data were obtained from steady-state currents like those shown in the upper panel plotted versus voltage. Continuous and dashed curves are the best fit of mean open probability (mean ± SE) obtained from at least eight experiments on KAT1 and KAT1-KAT1 channels, respectively.

TABLE 1 Half-activation potential and apparent gating charge of monomeric and dimeric constructs

Injection/coinjection	$V_{1/2}$ (mV)	z	N
$KAT1_{monomer}$	−121.9 ± 0.9	1.4 ± 0.7	7
$KAT1_{dimer}$	−123.4 ± 0.9	1.4 ± 0.6	7
a KAT1-KAT1:KDC1-KAT1	−176.2 ± 1.9	1.1 ± 0.4	6
b KAT1-KAT1:KDC1-KDC1	−204.7 ± 1.6	1.3 ± 0.4	7
c KDC1-KDC1:KDC1-KAT1	−207.6 ± 1.9	1.3 ± 0.5	6
d KDC1-KAT1	−206.4 ± 1.6	1.3 ± 0.5	9

Half-activation potential, $V_{1/2}$, and apparent gating charge, z, obtained from the best fit with Boltzmann distribution of the open probability of diverse monomeric or dimeric constructs injected ($KAT1_{monomer}$, $KAT1_{dimer}$, and injection **d**) or coinjected (coinjections **a**, **b**, and **c**) in *Xenopus* oocytes. N = number of experiments.

large inward-rectifying and robust currents (like those shown in Fig. 4 *A–C*) were observed. The currents elicited by tandem constructs were reminiscent of the currents of the heteromeric channels obtained by the coinjection of the monomeric KDC1 and KAT1 subunits. Indeed, the voltage activation characteristics of the KAT1-KAT1:KDC1-KAT1, KAT1-KAT1:KDC1-KDC1, and KDC1-KAT1:KDC1-KDC1 heteromeric channels changed significantly with respect to the homomeric KAT1 currents obtained by injecting either the KAT1 monomer or the KAT1-KAT1 dimeric construct, which was assumed as the control (Fig. 3 *A*).

From the Boltzmann fit of experimental data (in Fig. 4 *E*), we found the following values for $V_{1/2}$ and z:

$V_{1/2}(\mathbf{a}) = -176.2 \pm 1.9$ mV, $z(\mathbf{a}) = 1.1 \pm 0.4$ ($N = 6$) for coinjection **a**;
$V_{1/2}(\mathbf{b}) = -204.7 \pm 1.6$ mV, $z(\mathbf{b}) = 1.3 \pm 0.4$ ($N = 7$) for coinjection **b**;
$V_{1/2}(\mathbf{c}) = -207.6 \pm 1.9$ mV, $z(\mathbf{c}) = 1.3 \pm 0.5$ ($N = 6$) for coinjection **c** (Table 1).

It could be observed that by increasing the mean number of KDC1 subunits present in the injected constructs, the P_{open} characteristics shifted toward more negative membrane potentials while the activation kinetics slowed down (Fig. 4 *F*). In particular, very similar Boltzmann characteristics,

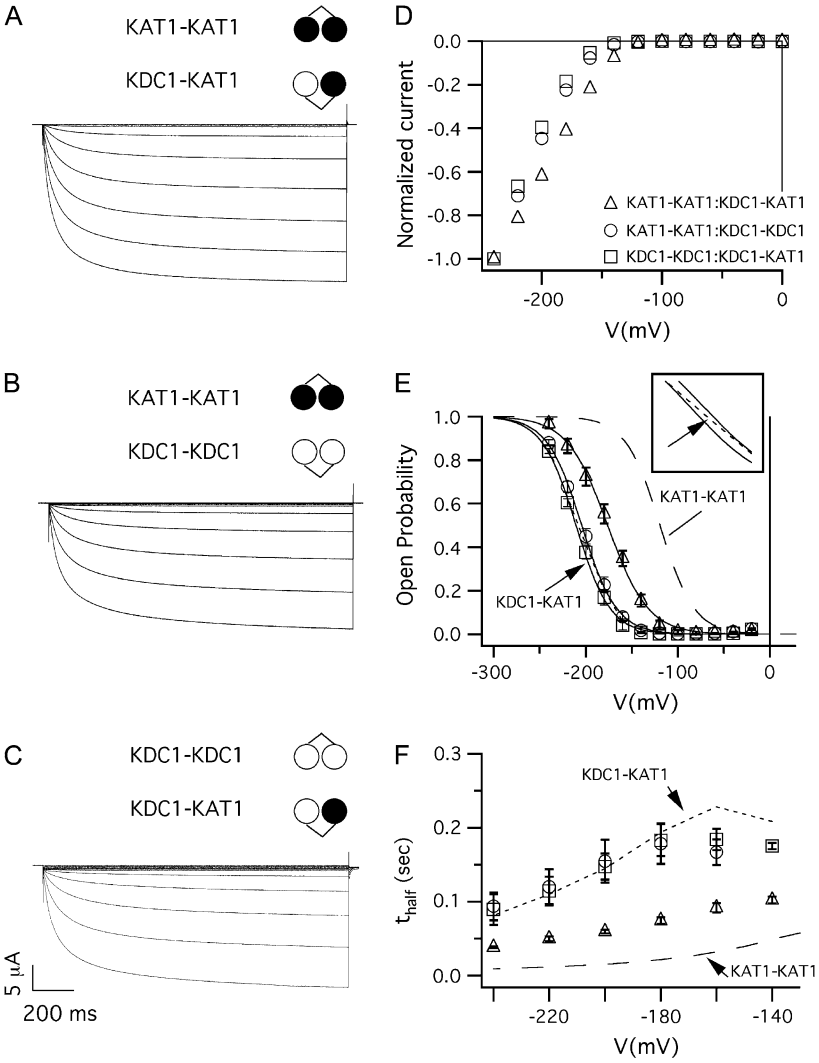

FIGURE 4 Current families, I–V, and kinetics characteristics of channels originated by coinjections of dimeric constructs. Ionic currents elicited by voltage steps from 0 mV to –240 mV in –20 mV decrements from a holding potential of 0 mV, in oocytes coinjected with the following tandem constructs at 1:1 weight ratio: (*A*) KAT1-KAT1 and KDC1-KAT1 (coinjection **a**); (*B*) KAT1-KAT1 and KDC1-KDC1 (coinjection **b**); and (*C*) KDC1-KDC1 and KDC1-KAT1 (coinjection **c**). (*D*) Current voltage characteristics of the current families shown in panels *A–C*, normalized with respect to the current at –240 mV. (*E*) Open-probability versus applied potential for the coexpressed dimers (mean ± SE, $N \geq 6$); continuous lines are the best fits with the Boltzmann equation of data from coinjections **a–c**; dashed line represents the homomeric KAT1-KAT1 channel and dotted line (indicated by the *arrow*) represents the currents mediated by KDC1-KAT1 channels (case **d1**); the inset shows a magnification of the Boltzmann curves for coinjections **b** and **c** and KDC1-KAT1 channels. (*F*) Half-activation times, $t_{1/2}$, of ionic currents plotted as a function of the membrane voltage. The symbols are the same as in panel *D*. Also, in this panel, the dashed line represents the half-activation times obtained from the homomeric KAT1-KAT1 tandem construct, while the dotted line corresponds to times produced by the KDC1-KAT1 dimer.

shifted by ≅ –80 mV with respect to KAT1-KAT1 (Fig. 4 *E*), were observed when the KDC1-KDC1 construct was coinjected with KAT1-KAT1 (coinjection **b**) or KDC1-KAT1 (coinjection **c**); on the contrary, whenever KAT1-KAT1 was coinjected with the KDC1-KAT1 dimer, the P_{open} characteristic was closer to the KAT1-KAT1 characteristics (*dashed line* in Fig. 4 *E*) displaying a smaller shift (i.e., ≅ −50 mV) (with respect to KAT1-KAT1) toward negative membrane potentials.

3KDC1/1KAT1 heteromers do not form functional channels

If all stoichiometric assemblies (except the one comprising 4 KDC1 subunits, see Fig. 3 *C*) contributed to the currents, then one should reasonably expect that the currents of the three channel cocktails (illustrated in Fig. 1) would display diverse activation kinetics, open probability, and response to zinc. Interestingly, the open probabilities of coinjections **b** and **c** were very similar to each other (the difference between $V_{1/2}$ of coinjections **b** and **c** was not statistically significant according to Student's *t*-test, $P > 0.1$). Moreover, they were comparable to those of channels comprising KDC1-KAT1 dimers only (case **d1**, see *dotted line* in Fig. 4 *E* and values in Table 1), which can only generate channels with an opposite KDC1-KAT1 symmetry. Furthermore, the activation kinetics of the currents in coinjections **b** and **c** almost coincided and were very close to those channels composed of KDC1-KAT1 dimers only, as shown in Fig. 4 *F*, where the values of the half-activation time, $t_{1/2}$, are compared. These similarities strongly support the hypothesis that the channels in **b** and **c** comprised a large percentage of 2KDC1/2KAT1 heterodimers.

Notably, a low percentage, or the absence, of KAT1 homotetrameric channels in case **b** was compatible with results reported in Fig. 2 *B*, where the presence of KDC1 strongly decreased the percentage of occurrence of homomeric KAT1 channels. These results were confirmed by the coinjection of the negative mutant dimer $KDC1_{G266A}$-$KDC1_{G266A}$ with KAT1-KAT1. Similarly to what was observed in Fig. 2 *B*, no inward currents were detected in 10 experiments, thus indicating a high affinity between KDC1-KDC1 and KAT1-KAT1 dimers (data not shown).

To further investigate the functional composition after different coinjections, we took advantage of the well-characterized zinc sensitivity conferred to heteromeric channels comprising KDC1 (20). We found that zinc had different effects on the ionic current of the diverse coinjections (Fig. 5). Zinc determined a systematic and significant increase of the currents produced by coinjections **b** and **c** (Fig. 5, *B* and *C*), i.e., at −160 mV $I_{Zn}/I_{control}(\mathbf{b}) = 1.9 \pm 0.1$ ($N = 7$) and $I_{Zn}/I_{control}(\mathbf{c}) = 1.9 \pm 0.2$ ($N = 6$), similarly to what had already been reported for injection **d** (Fig. 5 *D* at $V = -160$ mV $I_{Zn}/I_{control}(\mathbf{d}) = 1.8 \pm 0.1, N = 13$ (20)). Consistently, apart from their indistinguishable open probability and kinetics, coinjections **b** and **c** also displayed comparable responses to zinc.

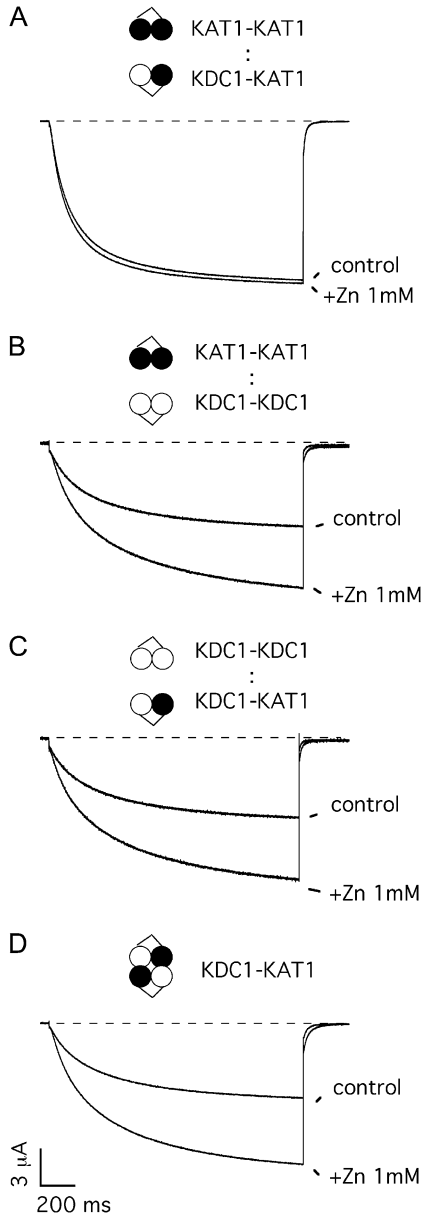

FIGURE 5 Zinc sensitivity of dimeric coexpressions. Typical potassium currents recorded in control solution and upon addition of 1 mM Zn^{2+} to solutions bathing oocytes coinjected with (*A*) KAT1-KAT1 and KDC1-KAT1 (coinjection **a**); (*B*) KDC1-KDC1 and KAT1-KAT1 (coinjection **b**); (*C*) KDC1-KDC1 and KDC1-KAT1 (coinjection **c**); and injected with (*D*) KDC1-KAT1 (injection **d**) tandem constructs. Holding potential and step potential were 0 mV and −160 mV, respectively.

We have previously demonstrated that histidine 224 (H_{224}) in the S5–S6 linker of KDC1 plays a crucial role in the modulation of the metal sensitivity of heteromeric KDC1-KAT1 channels (11). Channels formed by KDC1-KAT1 dimers, where H_{224} was mutated into alanine ($KDC1_{H224A}$-KAT1), did not display the usual KDC1-dependent zinc potentiation of the current (compare Figs. 5 *D* and 6 *A*). We took advantage of this property to investigate

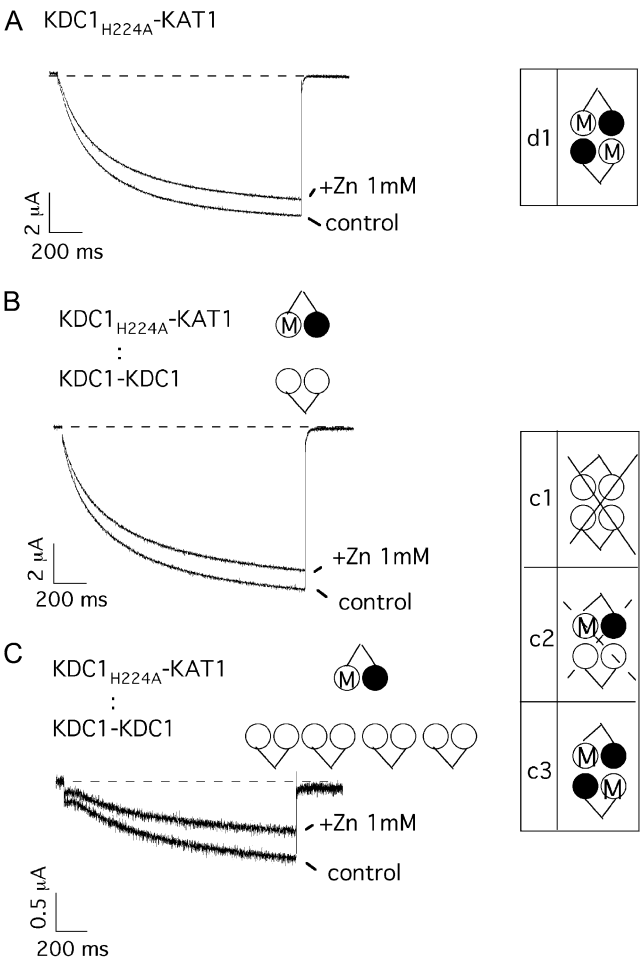

FIGURE 6 Mutation of histidine 224 removes zinc potentiation in coinjection **c**. (*A*) The addition of 1 mM external zinc to oocytes injected with the mutated tandem construct $KDC1_{H224A}$-KAT1 (equivalent to injection **d**) did not induce any current increase. Data are representative of over 15 experiments. (*B*) Also KDC1-KDC1 coinjected with $KDC1_{H224A}$-KAT1 at a cRNA ratio $R = 1{:}1$ did not show any current potentiation upon addition of external zinc to the bath. Data are representative of seven experiments. (*C*) The same coinjection at a fourfold higher KDC1-KDC1:$KDC1_{H224A}$-KAT1 ratio ($R = 4{:}1$) did not display any current potentiation, either. Data are representative of six experiments. Holding potential and step potential were 0 mV and −160 mV, respectively. Schemes at the right side illustrate the different possible cases of coinjection **c**. Crossed cases represent nonconductive configurations.

the functional properties of 3KDC1/1KAT1 channel. We demonstrated that the addition of $ZnCl_2$ to the bath solution determined a decrease of the ionic currents also when $KDC1_{H224A}$-KAT1 was coexpressed with the wild-type dimer KDC1-KDC1 (Fig. 6 *B*). If the heteromeric KDC1-KDC1/$KDC1_{H224A}$-KAT1 channel produced functional channels, then we should at least occasionally have observed an increase of the current upon addition of $ZnCl_2$, owing to the presence of two nonmutated KDC1 subunits in the channels. Actually, in nine experiments no increase of the ionic currents was observed upon addition of $ZnCl_2$. Furthermore, by increasing the ratio of injected KDC1-KDC1 to $KDC1_{H224A}$-KAT1 cRNA up to 4:1, coinjection **c** never displayed any current potentiation upon addition of zinc in five experiments (Fig. 6 *C*).

The amplitudes of the typical currents reported in Fig. 6, *B* and *C*, point out that the ionic currents decreased by increasing the percentage of injected KDC1-KDC1 cRNA. This confirms that, in coinjection **c**, the stoichiometric configuration comprising 3KDC1 and 1KAT1 was expressed but did not produce functional channels. Consequently, the only heterodimer contributing to the current in injection **c** is case **c3**, i.e., KDC1-KAT1/KDC1-KAT1.

Altogether, these results suggest that cases **c3** and **b2** are equivalent to case **d1**. This also indicates that the adjacent or opposite stoichiometric symmetry of the 2KAT1/2KDC1 channel does not affect channel functionality.

3KAT1/1KDC1 heteromers are functional channels

A comparison of diverse $V_{1/2}$ obtained from coinjection **a** as well as other coinjections (see Fig. 4 *E*) suggests that tetramers in **a** did not comprise only KDC1-KAT1/KDC1-KAT1 functional channels but also other stoichiometric configurations (Student's *t*-test confirmed that $V_{1/2}$ from coinjections **a** and **b** were significantly different with $P < 0.001$).

Moreover, the activation kinetics of currents recorded from coinjection **a** were significantly different from those of the other two coinjections (see Fig. 4 *F*); two typical traces produced by coinjection **b** and **c** were superimposed after normalization and reported in Fig. 7 *A*. The two traces coincided in accordance with the results illustrated above. In Fig. 7 *B* instead, the typical currents produced by coinjection **b** and **a** were compared at two appropriate potentials, taking into account the shift ($\Delta V \cong +30$ mV) in the voltage activation of these coinjections. The current of coinjection **b** was normalized (*dashed line*) and superimposed with that recorded from coinjection **a**. Consistently with $t_{1/2}$ vs. V (Fig. 4 *F*), the two current traces displayed significantly different activation kinetics. In Fig. 7 *C*, the current obtained by coinjection **a** (KAT1-KAT1:KDC1-KAT1) was compared with the current obtained by a linear combination (*dash-dotted line* indicated by the *arrowhead*) of the currents obtained from KAT1-KAT1 injection (*dashed line*) with KDC1-KAT1 injection (*dotted line*). The coefficients of the linear combination (obtained by means of a standard least-square procedure of current **a)** were 0.42 and 0.58 for the contributions of KAT1-KAT1 and KDC1-KAT1, respectively. Clearly, the experimental heteromeric current of coinjection **a** is significantly different from the KAT1-KAT1 and KDC1-KAT1 linearly combined currents, suggesting that the stoichiometric case **a2** also produced functional channels.

Further information could be obtained, in this case, by coinjection of tandem constructs at different cRNA weight ratios. Fig. 7 *D* shows the half-activation times for the

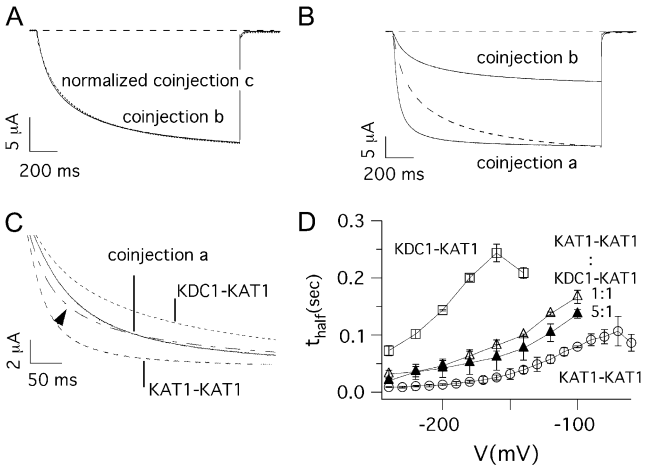

FIGURE 7 Kinetics of currents mediated by different dimeric coinjections. (*A*) Normalized currents measured at $V = -160$ mV in oocytes coinjected with KAT1-KAT1 plus KDC1-KDC1 (coinjection **b**) and KDC1-KAT1 plus KDC1-KDC1 (coinjection **c**). (*B*) The current measured at $V = -180$ mV in an oocyte injected with KAT1-KAT1 plus KDC1-KDC1 (coinjection **b**) was normalized and superimposed (*dashed line*) with that measured at the corresponding voltage $V = -150$ mV in an oocyte injected with KAT1-KAT1 plus KDC1-KAT1 (coinjection **a**). For a fair analysis of the kinetics, we compared two currents taken at voltages shifted by $\Delta V \approx 30$ mV to take into account the voltage shift of the Boltzmann distributions of the two coinjections. (*C*) Current traces recorded at −150 mV from an oocyte coinjected with KAT1-KAT1 plus KDC1-KAT1 tandem constructs (coinjection **a**), and from two distinct oocytes injected with KAT1-KAT1 ($V = -120$ mV), and KDC1-KAT1 ($V = -180$ mV) tandem constructs, respectively. The dash-dotted line (indicated by the *arrow*) represents the linear combination of KAT1-KAT1 homomeric current (*dashed line*) and KDC1-KAT1 heteromeric current (*dotted line*) and is superimposed to that obtained by KAT1-KAT1 plus KDC1-KAT1 coinjection. (*D*) Half-activation times (mean ± SE, $N \geq 8$) of ionic currents plotted as a function of the membrane voltage for KDC1-KAT1 (**d1**, *open squares*), KAT1-KAT1 (*open circles*) and coinjection **a** (KAT1-KAT1 plus KDC1-KAT1) at a cRNA ratio 1:1 (*open triangles*) and 5:1 (*solid triangles*).

KAT1-KAT1 dimer, the KDC1-KAT1 dimer and the coinjection of these two constructs at two different molar ratios KAT1-KAT1:KDC1-KAT1 = 1:1 and 5:1. If case **a2** (3KAT1/1KDC1) did not significantly contribute to current in **a** at a 5:1 (KAT1-KAT1:KDC1-KAT1) molar ratio, we should have expected values of the half-activation times very similar to those of the KAT1-KAT1 dimer; instead only a slight decrease of $t_{1/2}$ vs. V was observed with respect to 1:1.

Interestingly, in oocytes challenged with coinjection **a**, the mean value of the current upon addition of zinc did not change significantly with respect to the control ($I_{Zn}/I_{control} = 1.0 \pm 0.1$ at $V = -160$ mV; $N = 13$) (Fig. 5 *A*). This suggests that the functional channel population expressed by the oocytes in these conditions comprised another stoichiometry beside the 2KDC1-2KAT1 tetramers.

Finally, we verified that KAT1-KAT1 and $KDC1_{G266A}$-KAT1 (mutated coinjection **a**) produced functional channels (Fig. 8 *A*), which responded positively ($I_{Zn}/I_{control}$(**b**) $= 1.3 \pm 0.1$, $N = 13$) to zinc challenge (Fig. 8 *B*).

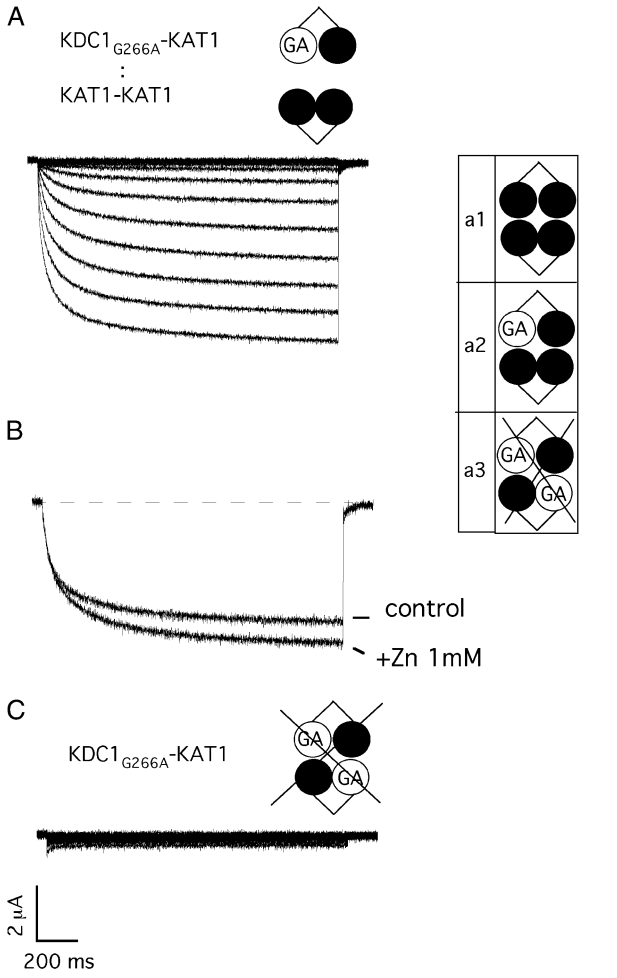

FIGURE 8 Heteromeric 3KAT1-1KDC1 channels are functional. (*A*) Ionic currents elicited by voltage steps from 0 mV to –240 mV in –20 mV decrements from a holding potential of 0 mV in an oocyte coinjected with the negative mutated tandem construct $KDC1_{G266A}$-KAT1 plus KAT1-KAT1. (*B*) External zinc (1 mM) potentiates current mediated by mutated coinjection **a**, $KDC1_{G266A}$-KAT1 plus KAT1-KAT1. Holding and step potential were 0 mV and −150 mV, respectively. (*C*) The mutated tandem $KDC1_{G266A}$-KAT1 in the KDC1 pore region does not produce currents up to –240 mV. The same results are obtained on different oocytes ($N = 15$). Schemes on the right side illustrate the different configurations used. Crossed cases represent nonconductive configurations.

Incidentally, this observation, together with the fact that the mutated dimer $KDC1_{G266A}$-KAT1 did not produce functional channels (Fig. 8 *C*), suggests that two mutations within the pore are incompatible with channel functioning, while one mutation is tolerated and produces functional 3KAT1/$1KDC1_{G266A}$ channels which respond positively to zinc.

DISCUSSION

KDC1 shows modulatory capability and high affinity for inward-rectifying K^+ channel subunits

In this article we revealed for the first time the functional properties of individual stoichiometric configurations of

heteromeric inward-rectifying potassium channels from plants expressed in *Xenopus* oocytes. Our attention was focused on the heteromerization of KAT1 and KDC1, investigating a series of tandem homo- and heteromeric constructs of these two subunits. Despite the fact that KAT1 and KDC1 derive from different plants (*A. thaliana* and *D. carota*) (26,39), they proved to be a convenient couple of subunits serving as a model system in heteromerization studies of plant K^+ *Shaker* channels: on the one hand, KAT1 is a well-characterized inward-rectifying potassium channel whose properties have been investigated for almost 15 years in several expression systems (29,40); on the other hand, KDC1 possesses peculiar properties that facilitate the monitoring of its presence in heteromeric channels (7,11,25). Indeed, KDC1 is a modulatory K^+ channel subunit, belonging to the silent plant *Shaker* channel group IV, which typically 1), favors the functionality of other inward-rectifying silent α-subunits in *Xenopus* oocytes; 2), slows down the activation kinetics of heteromeric channels; 3), shifts the threshold of channel activation toward negative voltages; and finally, 4), confers current potentiation to heteromeric channels upon zinc addition to the bath solution (7,11,25). Interestingly our approach, based on a combination of tandem constructs and KDC1 point mutations, demonstrated that KDC1 subunits have a very high affinity for other plant inward-rectifying potassium channels subunits: i.e., the presence of a KDC1 subunit (either in the monomeric or the dimeric form) prevented the formation of homomeric KAT1 tetramers (Fig. 2).

KDC1/KAT1 functional stoichiometry

Furthermore, we wondered whether the configurations 3KAT1/1KDC1, 2KAT1/2KDC1, and 1KAT1/3KDC1 constitute functional heteromeric complexes contributing to the macroscopic conductance of heteromeric KDC1/KAT1 channels. By analyzing the biophysical characteristics of coexpressed dimers (Fig. 4), the strong similarity between the open probabilities and the activation kinetics of channels produced by coinjections **b** (KAT1-KAT1:KDC1-KDC1) and **c** (KAT1-KDC1:KDC1-KDC1) are immediately noticeable. From the almost identical Boltzmann characteristics produced by these two coinjections and case **d**, it is plausible to draw up the following conclusions: in coinjection **b** only a small percentage of homomeric KAT1 channels were formed, and in coinjection **c** the combination of 3KDC1 and 1KAT1 subunits did not form functional channels (as demonstrated in Fig. 7). In this case, the stoichiometric composition of coinjections **b** and **c**, where **b2** and **c3** are the prevailing configurations, would be the same of the KDC1-KAT1 dimer (case **d1**). This possibility was strongly supported by the high affinity of the KDC1 dimer for the KAT1 dimer discussed above. Furthermore, a KDC1 mutation that abolished zinc-potentiation demonstrated that case **c2** was regularly formed but was not functional. Consequently, 2KDC1/2KAT1 channels comprising opposite (cases **c3** and **d1**) and adjacent (case **b2**) subunits had similar properties. When the pore-mutated construct ($KDC1_{G266A}$-KAT1) was coinjected with the KAT1-KAT1 construct, only the homotetrameric KAT1 (**a1**) and heteromeric (**a2**) 3KAT1/1$KDC1_{G266A}$ channels were functional, since the mutated configuration equivalent to case **a3** (2KAT1/2$KDC1_{G266A}$) produced electrically silent channels. Our results indicated that the 3KAT1/1KDC1 heteromer is a conductive channel. Furthermore, the small variation of $t_{1/2}$ (Fig. 7 *D*) after the fivefold increase of KAT1-KAT1/KDC1-KAT1 cRNA ratio, suggested that the presence of only one KDC1 subunit in the dimer was sufficient to significantly increase the formation of heteromeric 3KAT1/1KDC1 channels, with a consequent decrease in the occurrence frequencies of configurations **a1** and **a3**.

In coinjection **a**, differences in the zinc-response between heteromeric wild-type and pore-mutated 3KAT1/$KDC1_{G266A}$ were observed ($I_{Zn}/I_{control}(WT) = 1.0 \pm 0.1$ while $I_{Zn}/I_{control}$(mutant) $= 1.3 \pm 0.1$). This difference may be ascribed to a larger fraction of homomeric KAT1 channels when the wild-type tandem is used instead of the mutated (G266A) dimer. A plausible explanation may also reside in the different structure of the pore region induced by the G266A mutation. In KDC1/KAT1 heteromeric channels, the typical potentiation of the current observed upon Zn^{2+} addition to the bath solution is actually due to different mechanisms acting in parallel (11): 1), an increase of the current due to zinc binding to a specific site, located in the S3–S4 and S5–S6 linkers; and 2), missing current inhibition due to tyrosine 269 in the KDC1 pore, instead of histidine present in all other plant potassium channels (7,11,41). In KDC1, tyrosine 269 is located in the crucial pore region ^{264}GYGDLY, in close proximity to our mutation G266A, which produces electrically silent channels. Possibly, this pore mutation gives a further contribution to the relief of zinc block in KDC1 heteromeric mutated channels. This hypothesis is supported by the different behavior of heteromeric mutated channel with respect to homomeric KAT1 and heteromeric wild-type channel upon addition of nickel (data not shown). In fact, nickel reduces up to 50% of the KAT1 homomeric current, whereas, contrary to zinc, it typically induces only a reduced inhibition but no increase of the KDC1-KAT1 heterodimer current (11). It has been hypothesized that, in this case, the machinery responsible for current inhibition prevails with respect to current potentiation mechanisms. In the mutated coinjection 3KAT1/1$KDC1_{G266A}$, but not in the wild-type coinjection 3KAT1/1KDC1, Ni^{2+} induced a current enhancement (data not shown); this supports the hypothesis that, when the heteromeric pore carries just one G266A mutation, it becomes less sensitive to nickel binding and consequently current potentiation prevails.

This is a further proof that a KDC1 subunit participates in the pore of heteromeric KDC1-KAT1 channels (see (7)) and demonstrates that, while two subunits with a G266A

mutation are incompatible with channel functioning, one mutation in the pore affects the accessibility of divalent ions to the pore but does not jeopardize channel functionality.

CONCLUSIONS

Heteromerization capability of α-modulatory subunits investigated in animal voltage-gated channels showed some differences with our results. For example, a fixed 3:1 stoichiometry between α-subunits and modulatory α-subunit was observed both in Kv (13–15) and CNG channels (24). In Kv channels it has been shown that the formation of dimers of two modulatory α-values is very unlikely, whereas heteromeric and homomeric nonmodulatory dimers are expected to form readily. Our experimental conditions were rather different since the α-value tandems were artificially constructed. Consequently, we did not have information on the probability of dimer formation; nevertheless, our results indicated that the formation of a tetramer composed by two different homomeric dimers (KAT1-KAT1 and KDC1-KDC1) was highly probable. Moreover, when KAT1 and KDC1 monomers were coinjected in oocytes at 1:1 cRNA ratio, the currents were very similar to those expressed by KDC1-KAT1 tandem constructs, indicating that the 1:1 KDC1:KAT1 stoichiometry was preferred (13–15). Moreover, the 3KAT1/1KDC1 channel also resulted to be a functional heteromer. Therefore, in our working conditions, the coexpression with KAT1 of a plant potassium modulatory KDC1 subunit seems to give rise to different solutions with respect to animal channels, as KDC1 and KAT1 display a variable stoichiometry.

Possibly, like KAT1 does in oocytes, other endogenous *Shaker* subunits might cooperate with KDC1 in carrots to form heteromeric channels displaying activation and metal sensitivity characteristics, which depend on the properties of subunits participating in the channel.

We acknowledge the contributions of J. Scholz-Starke and P. Gavazzo, who both read the manuscript with a critical approach. English revision of the manuscript was by Paola Zucchi.

REFERENCES

1. Christie, M. J., R. A. North, P. B. Osborne, J. Douglass, and J. P. Adelman. 1990. Heteropolymeric potassium channels expressed in *Xenopus* oocytes from cloned subunits. *Neuron*. 4:405–411.
2. Isacoff, E. Y., Y. N. Jan, and L. Y. Jan. 1990. Evidence for the formation of heteromultimeric potassium channels in *Xenopus* oocytes. *Nature*. 345:530–534.
3. Ruppersberg, J. P., K. H. Schröter, B. Sakmann, M. Stocker, S. Sewing, and O. Pongs. 1990. Heteromultimeric channels formed by rat brain potassium-channel proteins. *Nature*. 345:535–537.
4. MacKinnon, R. 1991. Determination of the subunit stoichiometry of a voltage-activated potassium channel. *Nature*. 350:232–235.
5. Liman, E. R., J. Tytgat, and P. Hess. 1992. Subunit stoichiometry of a mammalian K^+ channel determined by construction of multimeric cDNAs. *Neuron*. 9:861–871.
6. Dreyer, I., S. Antunes, T. Hoshi, B. Müller-Röber, K. Palme, O. Pongs, B. Reintanz, and R. Hedrich. 1997. Plant K^+ channel α-subunits assemble indiscriminately. *Biophys. J*. 72:2143–2150.
7. Paganetto, A., M. Bregante, P. Downey, F. Lo Schiavo, S. Hoth, R. Hedrich, and F. Gambale. 2001. A novel K^+ channel expressed in carrot roots with a low susceptibility toward metal ions. *J. Bioeng. Biomembr*. 33:63–71.
8. Zimmermann, S., S. Hartje, T. Ehrhardt, G. Plesch, and B. Müller-Röber. 2001. The K^+ channel SKT1 is co-expressed with KST1 in potato guard cells—both channels can co-assemble via their conserved KT domains. *Plant J*. 28:517–527.
9. Formentin, E., A. Costa, M. Bregante, P. Gavazzo, A. Naso, C. Picco, F. Gambale, F. Lo Schiavo, and M. Terzi. 2003. KDC2: a novel carrot AKT1-like potassium channel. *In* International Congress of Plant Molecular Biology. Barcelona, Spain.
10. Dreyer, I., F. Poree, A. Schneider, J. Mittelstadt, A. Bertl, H. Sentenac, J. B. Thibaud, and B. Mueller-Roeber. 2004. Assembly of plant *Shaker*-like K_{out} channels requires two distinct sites of the channel α-subunit. *Biophys. J*. 87:858–872.
11. Picco, C., M. Bregante, A. Naso, P. Gavazzo, A. Costa, E. Formentin, P. Downey, F. Lo Schiavo, and F. Gambale, 2004. Histidines are responsible for zinc potentiation of the current in KDC1 carrot channels. *Biophys. J*. 86: 224–234.
12. Hille, B. Ionic Channels of Excitable Membrane, 3rd Ed. 2001, Sinauer, Sunderland, MA.
13. Hugnot, J. P., M. Salinas, F. Lesage, E. Guillemare, J. de Weille, C. Heurteaux, M. G. Mattei, and M. Lazdunski. 1996. Kv8.1, a new neuronal potassium channel subunit with specific inhibitory properties towards *Shab* and *Shaw* channels. *EMBO J*. 15:3322–3331.
14. Salinas, M., F. Duprat, C. Heurteaux, J. P. Hugnot, and M. Lazdunski. 1997. New modulatory α-subunits for mammalian *Shab* K^+ channels. *J. Biol. Chem*. 272:24371–24379.
15. Kerschensteiner, D., F. Soto, and M. Stocker. 2005. Fluorescence measurements reveal stoichiometry of K^+ channels formed by modulatory and delayed rectifier α-subunits. *Proc. Natl. Acad. Sci. USA*. 102:6160–6165.
16. Chen, T. Y., Y. W. Peng, R. S. Dhallan, B. Ahamed, R. R. Reed, and K. W. Yau. 1993. A new subunit of the cyclic nucleotide-gated cation channel in retinal rods. *Nature*. 362:764–767.
17. Korschen, H. G., M. Illing, R. Seifert, F. Sesti, A. Williams, S. Gotzes, C. Colville, F. Muller, A. Dose, M. Godde, L. Molday, U. B. Kaupp, and R. S. Molday. 1995. A 240-kDa protein represents the complete β-subunit of the cyclic nucleotide-gated channel from rod photoreceptor. *Neuron*. 15:627–636.
18. Sautter, A., X. Zong, F. Hofmann, and M. Biel. 1998. An isoform of the rod photoreceptor cyclic nucleotide-gated channel β-subunit expressed in olfactory neurons. *Proc. Natl. Acad. Sci. USA*. 95:4696–4701.
19. Bonigk, W., J. Bradley, F. Muller, F. Sesti, I. Boekhoff, G. V. Ronnett, U. B. Kaupp, and S. Frings. 1999. The native rat olfactory cyclic nucleotide-gated channel is composed of three distinct subunits. *J. Neurosci*. 19:5332–5347.
20. Picco, C., P. Gavazzo, and A. Menini. 2001. Co-expression of wild-type and mutant olfactory cyclic nucleotide-gated channels: restoration of the native sensitivity to Ca^{2+} and Mg^{2+} blockage. *Neuroreport*. 12:2363–2367.
21. Naranjo, D. 1997. Assembly of *Shaker* K^+-channels from random mixture of subunits carrying different mutations. *In* From Ion Channel to Cell-to-Cell Conversation. R. Latorre and J.C. Sáez, editors. Plenum Press, New York and London.
22. Ottschytsch, N., A. Raes, D. Van Hoorick, and D. J. Snyders. 2002. Obligatory heterotetramerization of three previously uncharacterized Kv channel α-subunits identified in the human genome. *Proc. Natl. Acad. Sci. USA*. 99:7986–7991.
23. Patel, A. J., M. Lazdunski, and E. Honore. 1997. Kv2.1/Kv9.3, a novel ATP-dependent delayed-rectifier K^+ channel in oxygen-sensitive pulmonary artery myocytes. *EMBO J*. 16:6615–6625.

24. Zheng, J., M. C. Trudeau, and W. N. Zagotta. 2002. Rod cyclic nucleotide-gated channels have a stoichiometry of three CNGA1 subunits and one CNGB1 subunit. *Neuron.* 36:891–896.

25. Formentin, E., S. Varotto, A. Costa, P. Downey, M. Bregante, A. Naso, C. Picco, F. Gambale, and F. Lo Schiavo. 2004. DKT1, a novel K^+ channel from carrot, forms functional heteromeric channels with KDC1. *FEBS Lett.* 573:61–67.

26. Anderson, J. A., S. S. Huprikar, L. V. Kochian, W. J. Lucas, and R. F. Gaber. 1992. Functional expression of a probable *Arabidopsis thaliana* potassium channel in *Saccharomyces cerevisiae*. *Proc. Natl. Acad. Sci. USA.* 89:3736–3740.

27. Schachtman, D. P., J. I. Schroeder, W. J. Lucas, J. A. Anderson, and R. F. Gaber. 1992. Expression of an inward-rectifying potassium channel by the *Arabidopsis* KAT1 cDNA. *Science.* 258:1654–1658.

28. Latorre, R., R. Olcese, C. Basso, C. Gonzalez, F. Munoz, D. Cosmelli, and O. Alvarez. 2003. Molecular coupling between voltage sensor and pore opening in the *Arabidopsis* inward rectifier K^+ channel KAT1. *J. Gen. Physiol.* 122:459–469.

29. Véry, A. A., and H. Sentenac. 2003. Molecular mechanisms and regulation of K^+ transport in higher plants. *Annu. Rev. Plant Biol.* 54:575–603.

30. Tu, L., and C. Deutsch. 1999. Evidence for dimerization of dimers in K^+ channel assembly. *Biophys. J.* 76:2004–2017.

31. Hedrich, R., O. Moran, F. Conti, H. Bush, D. Becker, F. Gambale, I. Dreyer, A. Kuch, K. Neuwinger, and K. Palme. 1995. Inward rectifier potassium channels in plants differ from their animal counterparts in response to voltage and channel modulators. *Eur. Biophys. J.* 24:107–115.

32. Sentenac, H., N. Bonneaud, M. Minet, F. Lacroute, J. M. Salmon, F. Gaymard, and C. Grignon. 1992. Cloning and expression in yeast of a plant potassium ion transport system. *Science.* 256:663–665.

33. Zimmermann, S., I. Talke, T. Ehrhardt, G. Nast, and B. Müller-Röber. 1998. Characterization of SKT1, an inwardly rectifying potassium channel from potato, by heterologous expression in insect cells. *Plant Physiol.* 116:879–890.

34. Hartje, S., S. Zimmermann, D. Klonus, and B. Müller-Röber. 2000. Functional characterisation of LKT1, a K^+ uptake channel from tomato root hairs, and comparison with the closely related potato inwardly rectifying K^+ channel SKT1 after expression in *Xenopus* oocytes. *Planta.* 210:723–731.

35. Nakamura, R. L., J. A. Anderson, and R. F. Gaber. 1997. Determination of key structural requirements of a K^+ channel pore. *J. Biol. Chem.* 272:1011–1018.

36. Heginbotham, L., and R. MacKinnon. 1992. The aromatic binding site for tetraethylammonium ion on potassium channels. *Neuron.* 8:483–491.

37. Gordon, S. E., and W. N. Zagotta. 1995. Subunit interactions in coordination of Ni^{2+} in cyclic nucleotide-gated channels. *Proc. Natl. Acad. Sci. USA.* 92:10222–10226.

38. Liu, D. T., G. R. Tibbs, and S. A. Siegelbaum. 1996. Subunit stoichiometry of cyclic nucleotide-gated channels and effects of subunit order on channel function. *Neuron.* 16:983–990.

39. Downey, P., I. Szabò, N. Ivashikina, A. Negro, F. Guzzo, P. Ache, R. Hedrich, M. Terzi, and F. Lo Schiavo. 2000. Kdc1: a novel carrot root hair K^+ channel: cloning, characterisation and expression in mammalian cells. *J. Biol. Chem.* 275:39420–39426.

40. Gambale, F., and N. Uozumi. 2006. Properties of *Shaker*-type potassium channels in higher plants. *J. Membr. Biol.* 210:1–19.

41. Hoth, S., I. Dreyer, P. Dietrich, D. Becker, B. Müller-Röber, and R. Hedrich. 1997. Molecular basis of plant-specific acid activation of K^+ uptake channels. *Proc. Natl. Acad. Sci. USA.* 94:4806–4810.